PHILOSOPHICAL TRANSACTIONS OF THE ROYAL SOCIETY A MATHEMATICAL, PHYSICAL & ENGINEERING SCIENCES

Saltation and Suspension Trajectories of Solid Grains in a Water Stream

J. E. Abbott and J. R. D. Francis

Phil. Trans. R. Soc. Lond. A 1977 **284**, 225-254
doi: 10.1098/rsta.1977.0009

SALTATION AND SUSPENSION TRAJECTORIES OF SOLID GRAINS IN A WATER STREAM

By J. E. ABBOTT and J. R. D. FRANCIS
Civil Engineering Department, Imperial College, London

(*Communicated by P. R. Owen, F.R.S. – Received 22 July 1975*)

CONTENTS

Vol. 284. A 1321. 29 [Published 18 February 1977

This paper continues the investigation of the motion of solitary grains in a water stream, reported by Francis (1973). The trajectories of solid grains are photographed by a multi-exposure technique as they are propelled by water streams along the bed of a laboratory channel. Many thousands of photographs were taken and analysed to determine the positions, velocities and accelerations of the grain. The technique does not take into account the possible effect, in multi-grain transport, of inter-granular collisions.

The three different modes of transport of grains were all observed – rolling, saltation and suspension, and the proportion of each found for a variety of transport stage u_*/u_{*0}. The development of suspension is much less rapid than the development of saltation from rolling, but even at the highest stage used, about 3.0, there is still a small amount of rolling. The trajectory dimensions and geometry are shown in relation to the stage which uniquely determines the geometry. Experiments where the grain is suddenly entrained from a stationary position show that several features of the subsequent trajectory are the same as those of a trajectory with a prior history of movement: thus it is inferred that the start of a trajectory is by way of hydrodynamic forces rather than by the conservation of momentum of previous trajectories.

Impacts and trajectories were analysed for the coefficient of friction $\tan\alpha$ and for the height of the effective thrust. While $\tan\alpha$ is shown to be rather larger than has been suspected in the past, the variation of y_n throws light upon predominance of slow fluid near the bed rather than high speed inrushes of fast fluid. Better information is now available for finding the mean forward speed of grains compared to that presented in the earlier paper. There are grounds for believing the existence of a 'shear-drift' force on grains when they are in a velocity gradient, giving a force opposing gravity: but there is no evidence of a proximity effect of the bed independent of the velocity gradient.

Notation

The stream:

u, v	stream velocities parallel to and normal to the bed
$\bar{u}$	time-mean stream velocity averaged over the whole depth
u', v'	instantaneous velocities due to turbulence
u_*	$= (\tau/\rho)^{\frac{1}{2}}$ shear velocity
u_{*0}	shear velocity at which grains start to move from a fully mobile bed
u_{*1}	shear velocity at which a grain over-riding on a fixed bed just starts to move
u_*/u_{*0}	transport stage
τ	fluid shear stress on the bed
ρ	fluid density
Y	depth of stream

The grains:

U, V	grain velocities parallel to and normal to the bed
$\bar{U}$	mean grain velocity averaged over several trajectories
V_g	terminal settling velocities of grains in still water
q	relative speed between grain and fluid
ρ_g	grain density
D	grain mean diameter
A	$= \frac{1}{4}\pi D^2$ grain cross-section area
θ_0	Shields parameter for the threshold of grain motion
C	coefficient of drag
F_x, F_y	drag forces in x and y directions

The trajectories:

t	time
T	overall time of one trajectory
x	distance along the bed
y	distance normal to the bed, from the mean level of the bed grain crests to the centroid of a moving grain
L	mean trajectory length
$y_{\max}$	maximum trajectory height
y_n	height of the effective thrust on a grain
x_1	distance from take-off, along the bed, to the crest of a trajectory
$\tan \alpha$	mean friction coefficient for intermittent contact with the bed
s	time interval between exposures
N	total number of intervals between images
overbars	denote averages over several trajectories
a, b, c, P, Q	constants defined in the text

1. Introduction

When studying the movement of irregularly shaped solid grains, such as sand, by water streams there is a need to analyse the motions of typical grains. Three different modes of transport can be easily seen: these are rolling in contact with the bed (when the fluid shear stress is only a little above the threshold value for any movement to take place at all); unsuspended motion, in a series of ballistic hops or saltations, controlled by the mean shear stress and bed roughness; and suspended motion, when grains move in generally longer trajectories, which appear to be slightly wavy, as the grain finds different local velocities in the turbulent stream. Eventually, at high water speeds and stresses, the grains follow a distinctly wavy path over very long trajectories. Unsuspended, and rolling modes occur near the bed, probably within a very few grain diameters, but suspended grains may be diffused into any part of the stream, the depth being the only limit to the trajectory height.

These modes, with their effect on the mean streamwise motion $\bar{U}$ of the grains, were described by Francis (1973), who simplified a fully mobile sand bed into a granular but fixed bed with one solitary grain of the same sort moving over it. This permits a much better visibility of a particular grain than is possible with a mobile bed, and to allow many features of its motion to be accurately observed through the side glass of a laboratory channel. A photographic method was described which gives a multi-image plate of the successive positions of a grain in a vertical plane, while it passes through the motion of all three modes. Typical trajectories have been shown as a Plate in Francis (1973).

The technique gives information about single grains, which do not modify the water stream properties. In a truly movable-bed stream, with a densely populated layer of moving grains, the water is retarded by the reaction of the hydrodynamic force driving the grains forward. Thus the speeds of and forces on grains found in the experiments to be described should not be indiscriminately applied to the practical engineering case. However, the general nature of the motions, and the significance of the various parameters measured are likely to have similarities in the two cases. In the absence of an experimental method to follow one grain in a

dense crowd of similar grains, the simplification may be acceptable in the present state of knowledge.

The 1973 paper had insufficient photographic information on which to base reliable statements about details of trajectories; and it is the purpose of this paper to describe an extensive series of simple experiments in which a large number of these photographs were analysed. The dimensions of, and velocities within the trajectories of grains; the mechanisms of the critical ejection from the bed and the later impact with it; the proportions of rolling, saltation and suspension occurring; the effect on the motions of stream depth Y: all of these when determined can throw light on the complex mixture of solid and fluid mechanics which occurs in sediment transport. Further consideration of $\bar{U}$, the mean forward speed of the grain, regarded as the integrated effect of many trajectories, can be given when details of these trajectories are known. The major parameter governing these variables will be taken to be the transport stage, u_*/u_{*0}. This useful parameter is defined as the ratio between the shear velocity u_* of the stream and the 'threshold' shear velocity u_{*0} at which grains just begin to move if they are part of a co-planar, fully mobile bed. At stages less than 1.0 there is no grain motion; at stages larger than 1.0 rolling, saltation and suspension can all occur. In the earlier paper (Francis 1973) the parameter used for this purpose was u_*/V_g; it was there shown also that $u_{*0} \propto V_g$ for a wide range of grain size, and providing the coefficient of drag of a grain C remained constant. Thus the stage and u_*/V_g are equivalent though of different numerical value. Later in this paper it will be shown that for purposes concerned with evaluation of $\bar{U}$, it is advantageous to use u_{*1} in place of u_{*0}, where u_{*1} is the shear velocity for grains to start moving if they are placed on top of, and so protrude above, a fixed bed. It is plain that $u_{*1} < u_{*0}$.

2. Experimental techniques and equipment – main series

All experiments were carried out in a straight, 30 cm wide, 12 m long glass-sided flume with a water supply from its own constant head tank. Rounded pea-gravel 4.8–9.6 mm sieve size was laid one grain thick as a plane bed, fixed in position with 'Feb' adhesive. No attempt was made to sort or to orientate the grains. The bed slope could be adjusted from horizontal to 0.0184, and the downstream control weir could be varied to give any required normal depth. The main part of the series was carried out at 4.8 cm depth Y with a smaller number of runs at 2.4, 7.2 and 9.3 cm depth. The measuring section was 6.5 m downstream of the start of the rough bed. The velocity profiles in this section were determined for a few runs, using a pitot-static tube. A typical profile is given in figure 15.

Three different moving grains were selected (two natural pea-gravel grains and one 6.3 mm diameter china sphere) as patterns to form a plaster-of-paris mould. Artificial grains were then cast from the mould with a mixture of lead filings and Araldite in different proportions so as to vary the specific gravity.

The properties of the grains are given in table 1. For each grain the Shields (1936) critical threshold shear velocity u_{*0} was calculated, as if the grain formed part of a plane bed of unfixed neighbours all similar to itself. The terminal settling speed V_g was measured by dropping grains into a large tank of still water and timing them over a given distance.

The grains were dropped singly into the water stream from above and 2 m upstream from the measuring point. They were photographed through the glass side of the flume by means of a multi-exposure technique with an electronic flash. A flash rate of 40 s^{-1} was used throughout.

The shear velocity of the stream u_* was derived from the bed slope and Y, no correction being made for the smooth side walls. In all tests care was taken to ensure a uniform Y along the whole length of the channel.

The positions x, y of the centroids of grains were digitized from the photographic images to a repeatable accuracy of 0.05 mm. The grain component velocities U and V over $\frac{1}{40}$ s intervals together with the accelerations were arithmetically derived. All computations were carried out on a CDC 6600 machine, the program being set up to identify a 'trajectory' of the grain even if it left the bed only for one flash, being flanked by two images both in contact with the bed. Further details of the experimental procedure can be found in Abbott (1974).

TABLE 1. PROPERTIES OF MOVING GRAINS

grain set	dimensions/cm	nominal diameter, D/cm	relative density and (terminal settling speed, V_g/(cm s^{-1}))					
1	0.642, 0.642, 0.642	0.642	1.20 (14.5)	1.26 (17.3)	1.43 (21.0)	2.07 (34.2)	2.88 (48.0)	2.49 (43.5)
2	1.080, 0.786, 0.630	0.828	1.20 (16.1)	1.24 (16.7)	1.43 (21.7)	1.80 (28.0)	—	2.57 (34.2)
3	1.400, 0.740, 0.580	0.882	1.20 (18.3)	1.28 (18.5)	1.54 (25.4)	1.76 (31.8)	2.86 (40.5)	2.60 (39.5)

3. TECHNIQUE AND EQUIPMENT – SUBSIDIARY EXPERIMENTS

A subsidiary experiment was arranged using the same 30 cm × 12 m long flume as the main series, to determine the trajectory of a solitary grain as it started from a stationary position on the bed. A movable grain was placed over a small hole in the fixed bed, and raised slowly into the water flow by a screw turned from below, the light flashing all the time. After some vibration the grain was suddenly plucked from the hole. The camera was operated with 1 s exposure, rapidly rewinding between each: by this means there was a better than 60 % chance of recording the start of a grain's trajectory. The chances of recording a whole trajectory are of course less than 60 %. Another subsidiary experiment was in a still-water tank. A series of high-speed cine records at 400 frames/s were made of the grains as they fell under gravity, starting from rest.

4. TRANSPORT MODES

At the beginning of this paper, rather crude definitions were given of the different modes. Now, with a great deal of data available on grain movements, more precision must be used to decide critically the mode of a particular trajectory. Therefore the following definitions, based on the method of analysis used, will be employed.

(i) Rolling mode: when the moving grain is in contact with the bed in successive photographic images. Note that a sliding motion is also included within the definition of rolling, and it is assumed that the moving grain is in contact with the bed for the time interval between successive images.

(ii) Saltation mode: when the moving grain jumps away from the bed and follows such a trajectory that its vertical acceleration is always directed downwards between the upward impulses sustained while in contact with the bed.

PHILOSOPHICAL TRANSACTIONS OF THE ROYAL SOCIETY A MATHEMATICAL, PHYSICAL & ENGINEERING SCIENCES

(iii) Suspension mode. Two slightly different views may be taken to define the onset of conditions when fluid impulses affect the trajectory. One, taken here, is to regard a trajectory as 'suspensive' when the vertical acceleration experienced by a grain, at any time between the upward impulses from the bed, is directed upward; thus a grain may experience an upward acceleration during the descending part of a trajectory even though its velocity is directed downwards throughout.

The above definition critically separates the saltant trajectories from those where fluid impulses first become effective, but it does not use 'suspended' in the common meaning of 'held up' or 'hung' – which presumably refers to position rather than to acceleration or velocity. The other view of suspension is that used by Bagnold (1973), which defines transport of a solid in suspension 'as that in which the excess weight of the solid is supported wholly by a random succession of upward impulses imparted by eddy currents of fluid turbulence moving upwards relative to the bed'. Bagnold then defines: 'Unsuspended transport may be distinguished as that in which no upward impulses are imparted to the solid other than those attributable to successive contacts between the solid and the bed.' This definition takes no account of the condition where vertically upward fluid impulses are exerted on the particle of strength and duration sufficient to overcome the gravitational force, but insufficient to reverse its downward momentum. Thus the important condition when turbulence just starts to affect grains is not specifically covered. In the present work, the limitations of equipment did not allow a sufficiently high u_*/u_{*0} to give a significant number of trajectories which are fully suspensive in the Bagnold (1973) sense.

Any one frame of the photographs may have in it several trajectories, not all in the same mode; and a collection of frames, all taken at the same stage, may disclose trajectories from all three modes.

(*a*) *Boundaries of modes*

The data from trajectories in 850 frames were searched for accelerations which define their mode, as above. At high stages there are 15–20 images per frame, and at the lower stages 35–40 images. After the mode is decided, the time between bed-contacts is assessed. Figure 1

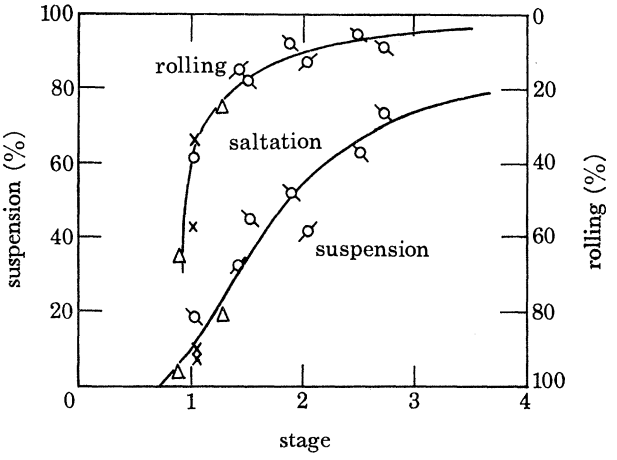

FIGURE 1. The bounds of transport modes of solitary grains in a water stream, as a function of stage, u_*/u_{*0}. Water depth 4.8 cm; grains of set 2 only. Information plotted from 385 photographs which include 716 trajectories. Note that percentage of time in rolling mode is increasing downwards; percentage of time in saltation then is represented by distance between curves. Points distinguished according to grain density, table 1, namely: ×, 2.57; △, 1.80; ♂, 1.43; ♀, 1.24.

shows the percentage of total time spent in each mode for a particular stage, each pair of points on the graph being the average for 35 frames. It is seen that the first points on the two curves appear slightly below a stage of unity. Since stage is defined in terms of u_{*0} which is loosely understood as that shear stress below which there is no grain movement, there appears to be a contradiction. The numerical values of u_{*0} used in plotting figure 1 were based on Shields parameter $\theta = 0.06$. It must be remembered that Shields experiments were carried out with co-planar beds and that the criterion for the onset of particle movement is very much at the discretion of the individual experimenter. Further, all of the present series were carried out by dropping the moving grain into the flow from above. It then immediately became an over-riding grain protruding into the flow far above the mean level of the top of the fixed bed particles. It has been shown, in a separate series of experiments as yet unpublished, that protrusion greatly decreases the shear stress required to cause motion. Therefore, it is not surprising that motion was recorded with overriding grains below a stage $u_*/u_{*0} = 1.0$. However, at stages < 1.0, whenever the grain found a hole between bed particles so that it became co-planar with them, its motion stopped and would not subsequently be restarted by the stream.

(*b*) *Accelerations during suspensions*

In a trajectory, after the initial upward acceleration (take-off), the grain has on it a steady downwards vertical acceleration due to gravity, and a variable vertical acceleration due to fluid forces on it. By definition, a suspensive trajectory must have at least one point where the resultant acceleration is directed upwards. It is therefore of interest to determine the frequency of occurrence and magnitude (averaged over two time intervals of $\frac{1}{40}$ s) of these upward accelerations, and so to have some information about the effects of fluid turbulence.

Three typical runs have been selected, within which all trajectories were searched for upward accelerations, excluding those associated with the first image after the grain left the bed (where the velocity could not be determined since the instant of leaving the bed is unknown). In the saltations there were, of course, no upward resultant accelerations at all. The frequency of each group of values of accelerations is shown in figure 2, the number of occasions being

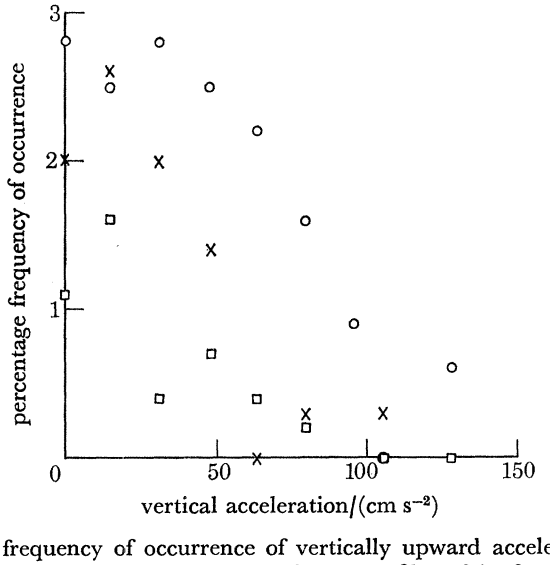

FIGURE 2. Magnitude and frequency of occurrence of vertically upward accelerations during trajectories for three different stages. Information for each stage from one film of 35 frames. Number of time intervals searched was 321, 345 and 449 for stage 2.52 (○), 1.53 (×) and 1.43 (□), respectively.

standardized by the total number of time intervals (in saltations and in suspensions) which were searched. For each run, there is a large scatter of the points due to the relatively small population from which the frequency is obtained; and this shows the great amount of photographic data needed to obtain conclusive frequency diagrams. At the highest stage, 2.52, four accelerations were found which exceeded 120 cm/s², one going as high as 240 cm/s². Without sufficiently smooth frequency curves, it appears valueless to standardize the acceleration variable of figure 2 by some parameter appropriate to the water stream; but the three plots show that the frequency of occurrence of upward accelerations increases with u_*/u_{*0}.

5. Statistics of trajectories

The coordinate data were searched for complete trajectories and for incomplete trajectories which included a crest. Measurements of the following kinds were taken and are plotted against u_*/u_{*0} in figures 3–8: mean maximum height $\bar{y}_{max}$ and mean length $\bar{L}$ of saltant and of suspensive trajectories, according to the definitions of §5; mean $\bar{y}_{max}$ and $\bar{L}$ of all trajectories; mean height of grains above the bed during the entire motion; the distribution of y_{max}

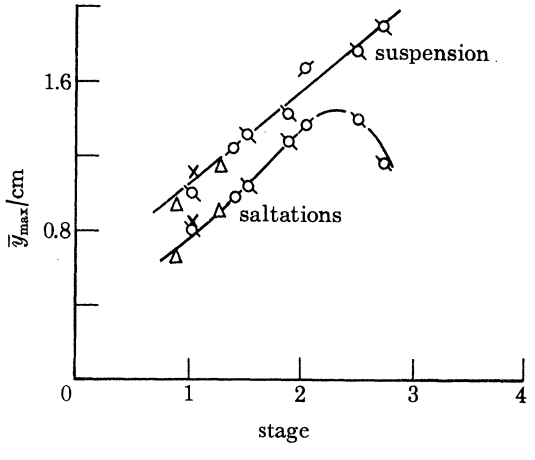

Figure 3

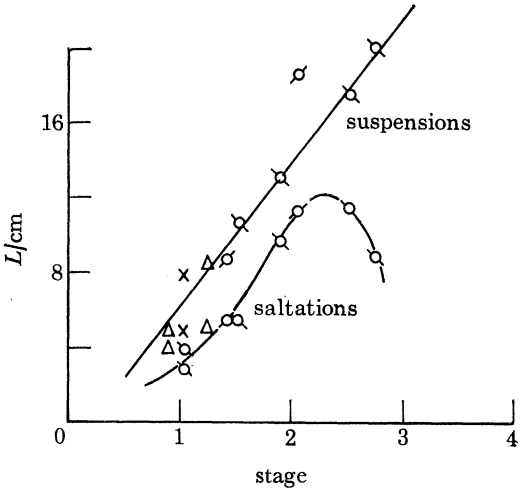

Figure 4

Figure 3. The mean maximum heights of trajectories, $\bar{y}_{max}$ subdivided into saltations (lower curve) and suspended motions (upper curve). Water depth 4.8 cm; grains of set 2 only. Information from 385 photographs which include 467 saltations and 249 suspensive trajectories. Point notation as in figure 1. Rolling is not considered a trajectory and so is ignored in finding these mean values of y.

Figure 4. The mean length $\bar{L}$ of trajectories subdivided into saltations (lower curve) and suspended motions. Water depth 4.8 cm; grains of set 2 only. Information from 385 photographs which include 371 saltations and 171 suspensive trajectories. Point notation as in figure 1.

for all trajectories at a particular stage; and the ratio y_{max}/L for all trajectories at the same stage; with saltant and suspensive trajectories discriminated. We draw attention to the way in which we have not made non-dimensional ratios for y or L. Since the grain diameter D seems the only practical dimension available for the purpose, and since it is constant at $D =$ 8.28 mm for all these results, it would give a false impression of generality to plot y_{max}/D or L/D in thefigures. Nevertheless we think it highly likely that this method of non-dimensionalizing would be effective with a wider range of data.

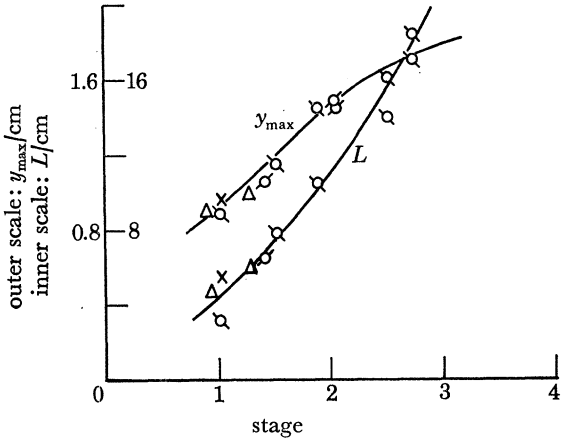

FIGURE 5. Average heights y_{max} and lengths L of all trajectories (suspensive and saltant), from 385 photographs, including 716 trajectories for height and 542 for length. Stream depth 4.8 cm; set 2 only. Point notation as figure 1.

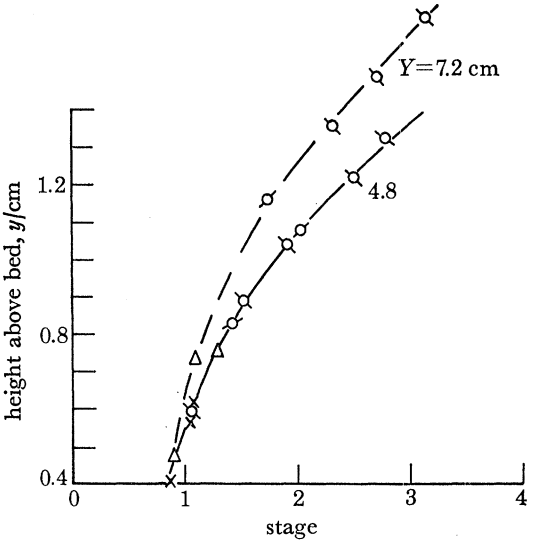

FIGURE 6

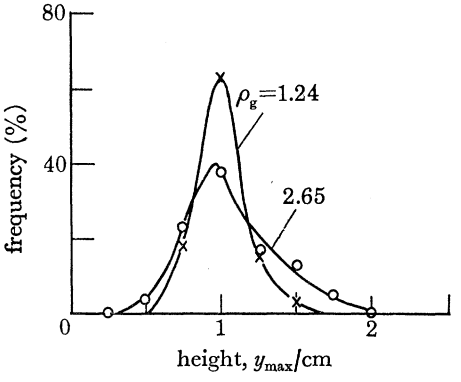

FIGURE 7

FIGURE 6. Average height of *all* positions of grains throughout trajectories including rolling. Set 2 only; stream depths 4.8 and 7.2 cm. Information from 8455 positions for 4.8 cm; 3305 positions for 7.2 cm. Point notation as figure 1. A grain in contact with the bed would have $y = 0.41$ cm.

FIGURE 7. Distribution of y_{max} of trajectories at a low stage, for grains of set 2 but of two different ρ_g. Information from 171 trajectories for $\rho_g = 2.65$ (○); from 65 trajectories for $\rho_g = 1.24$ (×).

Two other statistics concerned with the mechanics of movement were determined from some of the data. These are y_n, the height of the centre of fluid thrust (Bagnold 1973) and $\tan\alpha$, the coefficient of effective friction. Their derivation is given in the appendix, and it is clear that both are dependent on knowing the precise time during which a grain is in trajectory above the bed. To improve this precision of finding both N, the number of flash intervals between grain take off and landing, and the grain velocities at these positions, a quadratic extrapolation was used on the three successive grain-images at each end of the trajectory. Such a method assumes that the acceleration is uniform over the two flash-intervals between the images. To avoid errors from rapidly changing accelerations, it was decided to limit

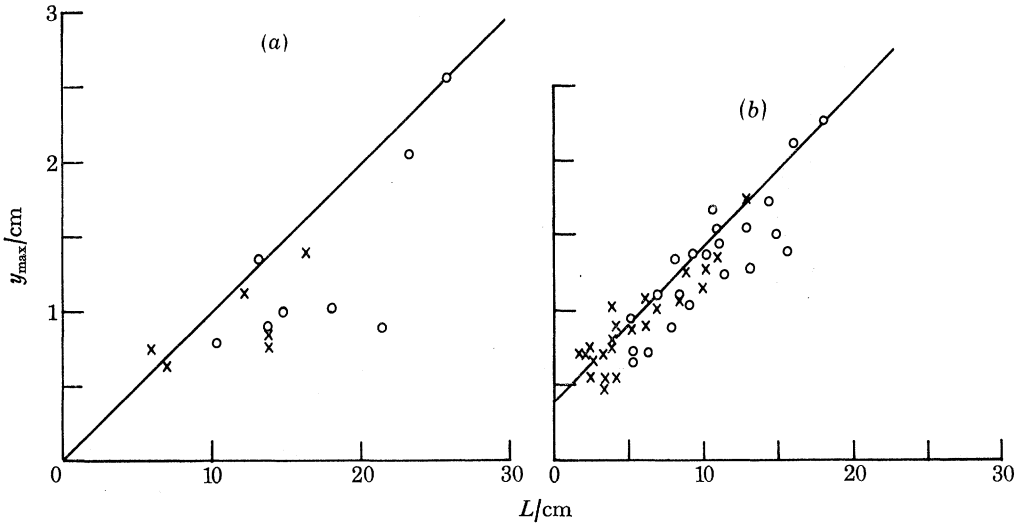

FIGURE 8. Trajectory dimensions at two different stages for set 2 grains, circles being suspensions, crosses being saltations. (*a*) $u_*/u_{*0} = 2.52$; information from 14 trajectories; (*b*) $u_*/u_{*0} = 1.53$; 45 trajectories.

analysis to those trajectories of 6 intervals or longer (i.e. 0.15 s and above). Thus the derived statistics for y_n and tan α are systematically biased towards longer trajectories.

The analysis for y_n was therefore done for the 30 longest trajectories of run 70, $u_*/u_{*0} = 1.53$. The wide differences between trajectory velocities leading to a wide scatter in the 30 values of y_n are shown on figure 9*a* and *b*. There is a similar scatter in values of tan α, as shown for the same 30 trajectories in figure 10; however there is a trend showing an increase of tan α for smaller trajectories (smaller N and T), and this must be borne in mind for the mean values in 4 runs as given in table 2.

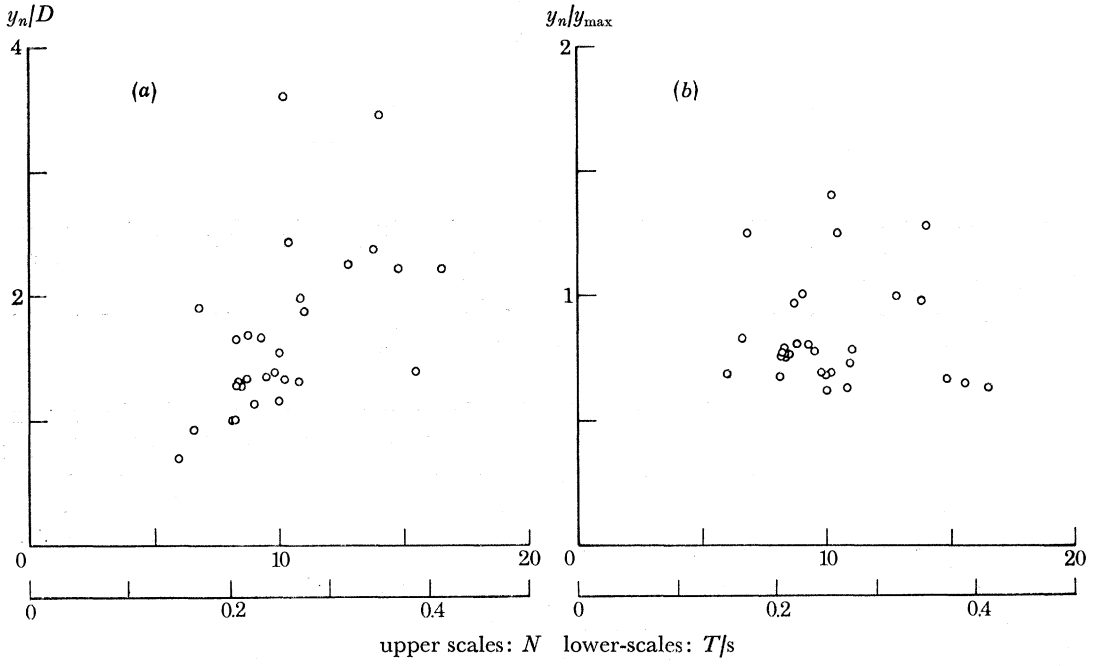

FIGURE 9. The statistics of y_n from 30 trajectories at $u_*/u_{*0} = 1.53$. (*a*) y_n/D for different times T of the hole trajectory; (*b*) y_n/y_{max} for different T. Observe several values > 1.0.

TABLE 2. MEAN VALUES OF tan α

number of trajectories	stage	tan α
8	0.91	0.38
30	1.53	0.42
10	2.52	0.62
11	2.74	0.71

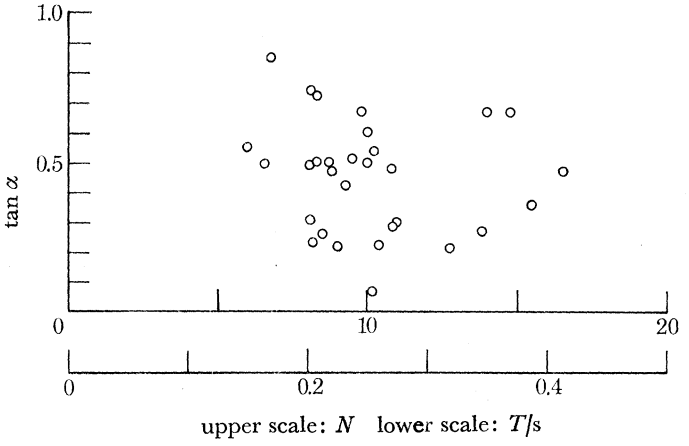

FIGURE 10. Variation of tan α with time T of trajectory for 30 trajectories at $u_*/u_{*0} = 1.53$.

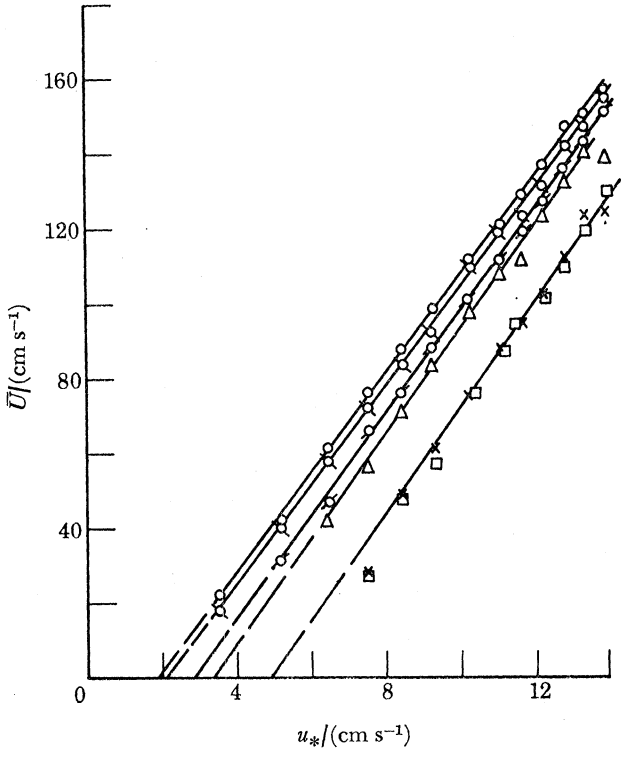

FIGURE 11. Mean forward speed $\bar{U}$ for set 3 grains at different densities. Stream depth 4.8 cm. Grain density: ○, 1.20; ◔, 1.26; ◴, 1.54; △, 1.76; ×, 2.86; □, 2.60.

The tests for $\bar{U}$ were carried out with far better control of depth Y than was done for the preliminary experiment of Francis (1973). At the same Y, $\bar{U}$ formed a closely linear function of u_*, with grains (all of the same shape) of different densities falling on different lines. Figure 11 shows a typical set of results for the set 3 grains over the range $1.20 < \rho_g < 2.86$. There does not appear to be much deviation from the straight line as the grain gradually changes its mode from rolling, through saltation to suspension.

Another useful analysis is to see if the mean U for grains when in trajectories (saltant and suspensive) is different from that of the rolling part of the total movement. Three runs were selected so that u_*/u_{*0} were nearly the same. Each digitized record was divided into trajectory lengths and rolling lengths and mean forward speeds found as table 3.

There is clearly little difference in the ratios shown despite differences in shape and ρ_g, thus solid friction, as grains roll or slide in portions of the travel, which might greatly change $\bar{U}$ for rolling, does not appear to affect $\bar{U}$ to any marked extent.

TABLE 3. MEAN $\bar{U}$ SEPARATED INTO TRAJECTORY AND ROLLING MODES

stage	grain	ρ_g	$\bar{U}_{traj}$	$\bar{U}_{roll}$	$\bar{U}_{roll}/\bar{U}_{traj}$
2.07	set 3 (sphere)	1.26	42.2	33.5	0.79
2.06	2	1.43	64.0	48.9	0.76
2.52	2	1.24	62.7	45.9	0.73

6. GRAIN SHAPE AND STREAM DEPTH EFFECTS

(a) *Grain shape*

Although the results of §§4 and 5 have been presented for the special case of set 2 grains a number of runs were made and the photographs analysed in the same way, using grains of sets 1 and 3. These were a sphere set 1, and the models of a piece of rounded gravel set 3, of which the length is twice the minimum dimension. The latter was one piece which had been picked from the sample of gravel forming the bed, and was probably near the extreme shape to be found therein.

The data from the analyses were plotted as was done in figures 1–6 for the set 2 grains; they are not reproduced here, because the experimental points fall so close to the points taken with the no. 2 set, no point being further than 2% away. It therefore appears that the effect of changing the shape of the moving grain, provided it falls within the range of shapes in the sample of the bed, makes very little difference to the trajectories. It should be borne in mind, however, that if moving grains are used of a grossly dissimilar shape to those in the bed sample, then very different results may be expected. Also, if both bed and moving grain are different in shape from those of the present sample, then considerable variations of the trajectory statistics are likely, as was experienced when the mean speed $\bar{U}$ was determined (Francis 1973). However, very angular grains are unlikely to be found in real rivers, since sharp corners are rapidly worn away.

(b) *Depth Y*

While most runs were made at $Y = 4.8$ cm depth, a less extensive series was made at $Y = 7.2$ cm. One aspect of this change has already been described in figure 6. Other statistics of the motion are shown together in figure 12, where the firm lines are those of the results of the main series, but the points are those for $Y = 7.2$ cm. It will be seen that $\bar{L}$ is larger for

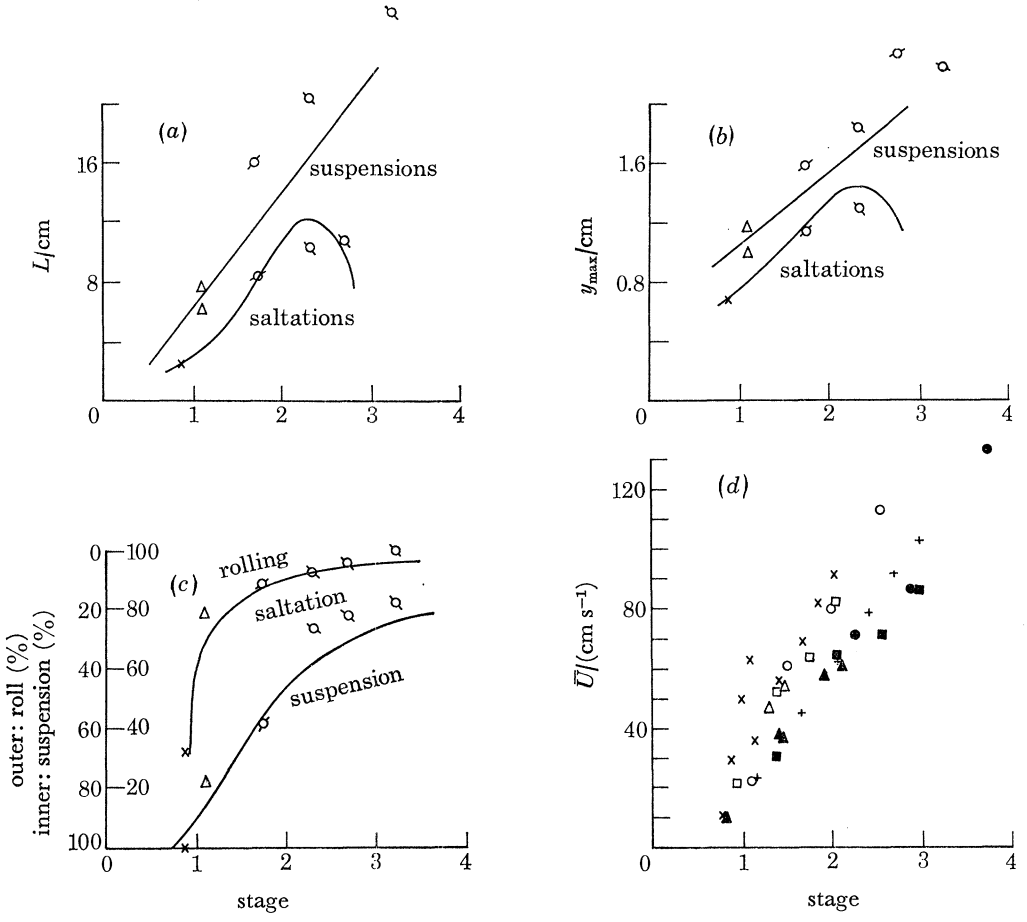

FIGURE 12. Effect of changing the stream depth Y on the properties of trajectories. In figures (*a*), (*b*) and (*c*) the solid lines are drawn for $Y = 4.8$ cm depth (i.e. identical to figures 4, 3 and 1 respectively). The individual points refer to the same grains, but in a stream of $Y = 7.2$ cm.

(*a*) Mean length of trajectories subdivided into saltations and suspended motions. Information from 320 photographs, which include 136 saltations and 61 suspensive trajectories.

(*b*) Mean y_{max} subdivided into saltations and suspended motions. Information from 320 photographs, which include 202 saltations and 138 suspensive trajectories.

(*c*) The bounds of transport modes. Information from 210 photographs which include 320 trajectories.

(*d*) Mean forward speed $\bar{U}$ as a function of u_*/u_{*0}. Each point represents the mean of 10 runs each over a distance of 5.512 m.

symbol	grain density	stream depth/cm
X	1.43	4.8
○	1.43	9.2
□	1.43	7.2
△	1.43	2.4
+	1.24	4.8
■	1.24	7.2
●	1.24	9.2
▲	1.24	2.4

the suspensive trajectories at the greater depth, though it is about the same for saltations; and that $\bar{y}_{max}$ is somewhat greater (perhaps 5%) for suspensions, but about the same for saltations. Study of the mode occurrence figure 12*c*, shows that the larger depth gives about the same occurrence of rolling as at the smaller depth, but that suspensions at the higher stages are distinctly more frequent. Thus it appears evident that the greater depth at the same

stage allows more frequent suspensions, which carry the grains to a somewhat greater height; but that when grains are not subjected to suspensive forces, and they merely saltate, then depth changes do not affect them. The mean forward speed $\bar{U}$ of the grains is shown in figure 12*d*. This is the statistic given by Francis (1973), and indeed some of the data points in the figure appeared in that reference: the presentation is, however, rather different. For any one value of ρ_g, $\bar{U}$ depends on stage and Y is unimportant. At other ρ_g, there is a different $\bar{U}$ to u_*/u_{*0} relation, but Y is not involved.

7. Statistics of impacts

The coordinate data of the main series have been used to find information about the impacts between trajectories. Frames were searched for cases where the grain is visible for as few images before and a few after the impact. They were then examined to see how often the grain rolled in contact with the bed for a short time before it again started a trajectory. Run 70, $u_*/u_{*0} = 1.53$ is typical of many other runs; 59 impacts were seen; 5 only were certainly seen to have a clear rebound devoid of rolling. A further 4 impacts were seen where there only appeared to be one image in contact with the bed, but subsequent quadratic extrapolation (see § 5) of the coordinates before and after impact revealed that there may have been a short unobserved roll of time duration $< \frac{1}{40}$ s between the landing and take-off. Of the 59 trajectory landings, 45 showed the grain in contact with the bed for 2 more consecutive images. In 5 impacts there was insufficient length of record, because of the frame limits, to determine the possibility of rolling. The distribution of the extent of the rolling is given in table 4, where 0 implies that only one image was seen in contact with the bed.

Table 4. Distribution of roll duration in contact with the bed following an impact at $u_*/u_{*0} = 1.53$

($\frac{1}{40}$ s interval)

roll duration	0	1	2	3	4	5	6	7	8	9	10	11
no. of occurrences	14	15	11	12	3	1	0	1	0	1	0	1

In addition, these impacts were studied for the vertical velocity V immediately after the beginning of the subsequent trajectory. The quadratic extrapolation was again used, so the trajectory must have a least 6 flash intervals in it. The 5 'clear' impacts averaged $V = 17.6$ cm/s; the 4 'short roll' impacts averaged 20.3 cm/s. The same record, studied without quadratic extrapolation (and thus taking smaller trajectories into account) gave for the first clear interval seen: $V = 14.3$ cm/s for 'clear' impacts; $V = 12.6$ cm/s for all other impacts.

It seems that clear rebounds, without rolling, are rare; and that most take-off velocities at the start of a trajectory are uninfluenced by the previous impact.

8. Subsidiary experiments

(*a*) *Grains starting from rest*

The paths of grains as they started a trajectory from rest were compared to trajectories of the main series at the same u_*/u_{*0}, but which had started from an impact at the end of the previous trajectory. The experimental difficulties led to many starts of these trajectories being

lost, and sometimes the final impact point was not seen. Results from analyses of the 'from-rest' trajectories, compared with corresponding information from main series trajectories are given in table 5, where x_1 is the distance from the starting point to the crest.

TABLE 5. DIMENSIONS OF TRAJECTORIES WITH GRAIN STARTING FROM REST

	u_*/u_{*0}	y_{max}/cm	$\frac{x_1}{y_{max}}$	$\frac{L}{y_{max}}$
main series, run 60	2.057	1.643	4.2 (32 obs.)	9.77 (21 obs.)
from rest	2.167	1.505	2.58 (12 obs.)	5.98 (6 obs.)
main series, run 70	1.532	1.231	2.73 (30 obs.)	6.79 (23 obs.)
from rest	1.623	1.428	1.98 (13 obs.)	5.32 (4 obs.)

Since the experimental restrictions result in many of the longer trajectories being cut off, $\bar{L}$ is likely to be underestimated in the 'from-rest' trajectories. The main series trajectories (which for this purpose excluded the very smallest) have a somewhat similar distortion, for there are more of them having a visible crest (and so y_{max}) than there are with a visible beginning and ending.

(*b*) *Vertical displacements*

The y–time curve for grains in still water, while accelerating from rest, has been compared to the y–t curves for grains falling from trajectory crests in the water stream. Two such comparisons (of many) are shown in figure 13. To demonstrate the variability from one trajectory to another, at the same u_*/u_{*0}, all complete trajectories of one film have been presented. Apart from irregularities clearly caused by bursts of turbulence, the records from the higher trajectories, show only small variables from the still water curve. In the lower trajectories, the y–t curves all appear above that for the still-water case.

9. DISCUSSION

(*a*) *Hydrodynamic lift and drag forces*

The forces acting on a grain govern the shape and properties of the resulting trajectory. As pointed out by Bagnold (1973), a solution of the equations of motion of a grain to determine drag or lift coefficients is of academic interest only. Such analysis could not determine the relative magnitude of a number of body forces present, all of which might produce the observed grain accelerations. Furthermore, many trajectories would need to be analysed from our data which, with $\frac{1}{40}$ s intervals, is rather coarse for the rapidly varying accelerations. One trajectory, analysed in detail in Abbott (1974), is shown in figure 14, with its velocity components. The velocity around the grain $(u-U)$ varied from -42.6 to $+3.0$ cm/s, while the resultant relative velocity of the grain $q = ((u-U)^2+V^2)^{\frac{1}{2}}$ varied from 52.3 to 12.3 cm/s An indication of the order of magnitude of the total horizontal and vertical forces F_x and F_y which must have been experienced to result in the measured accelerations are $-0.006 < F_x < +0.293$ gf, while $-0.209 < F_y < +0.025$ gf on the grain which had a submerged weight of 0.036 gf. It should be noticed that estimates of F_x and F_y must be determined by reference to q and the angle arctan (V/U) as hinted by Bagnold (1973) and not solely by the squares of the velocity components. The velocity u, and gradient $\mathrm{d}u/\mathrm{d}y$ are given in figure 15.

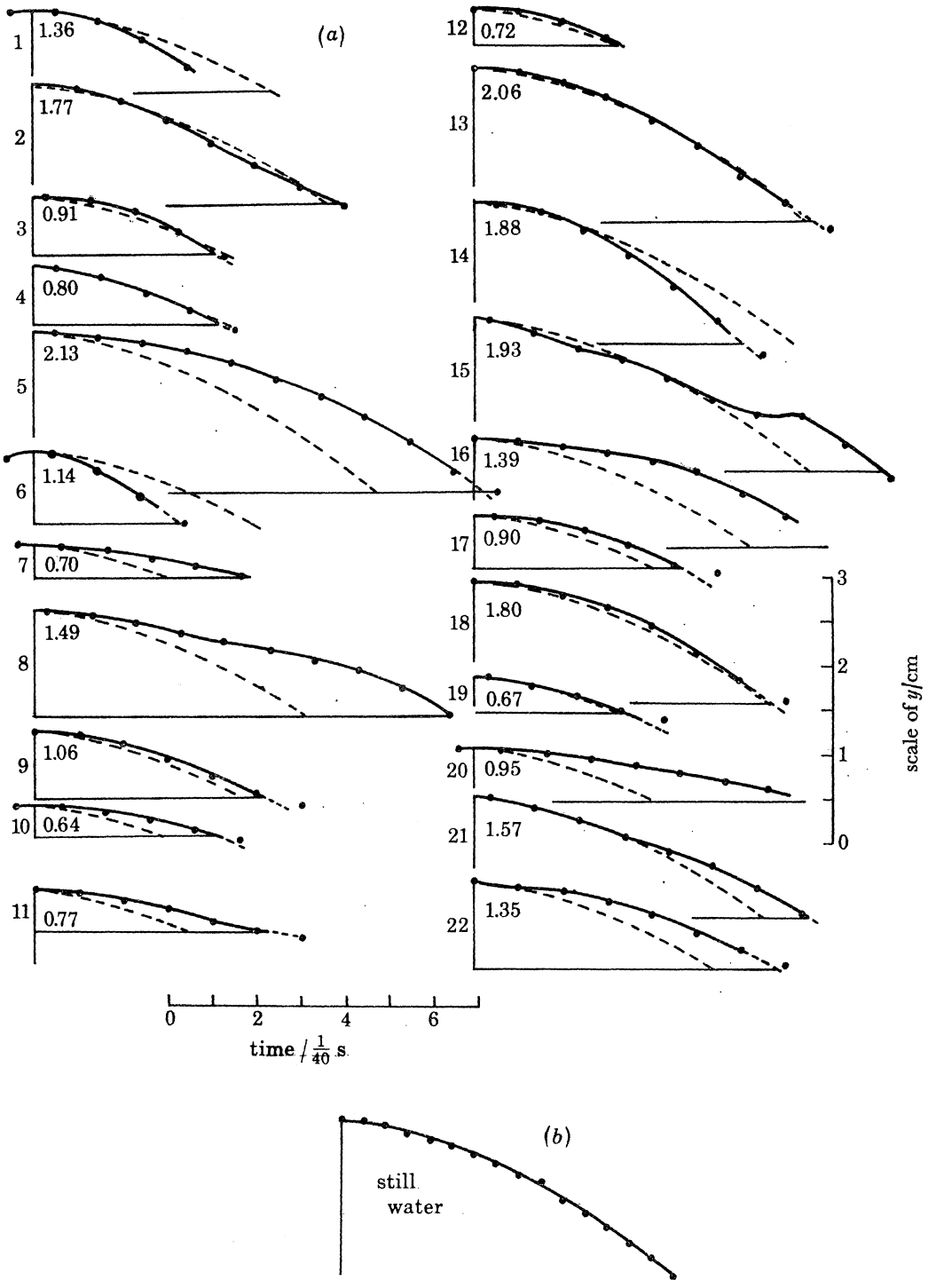

FIGURE 13. (*a*) Vertical displacement downwards from crest of 22 trajectories; main series experiments; sphere at $u_*/u_{*0} = 2.07$. Numbers against left-hand ends of curves indicate the height (cm) of the crest of the trajectory. Dotted line shows still water displacement curve. (*b*) Vertical displacement of grains falling from rest in still water, to the same scales.

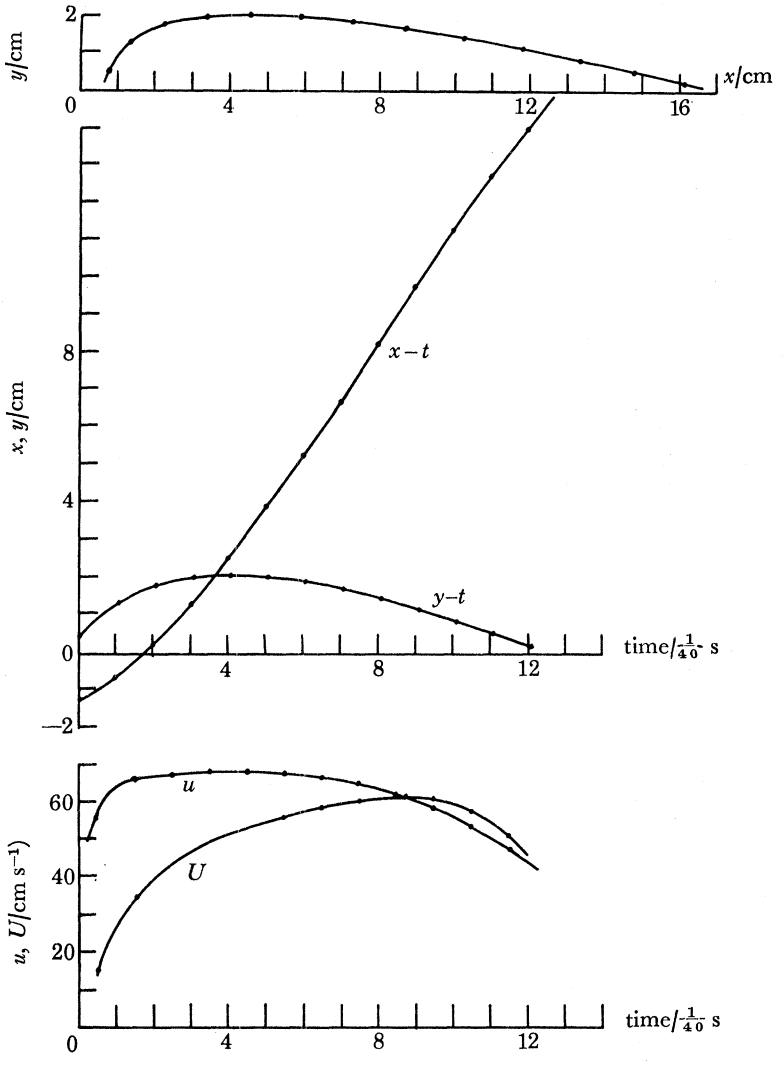

FIGURE 14. Grain motion in a selected but typical trajectory $u_*/u_{*0} = 2.07$; of a sphere of $\rho_g = 1.26$. (*a*) Grain path: coordinate positions, x and y, at $\frac{1}{40}$ s intervals. (*b*) x and y function of time. (*c*) Horizontal velocity of the grain U superimposed over the time-mean horizontal velocity of the stream u at the instantaneous height y of the grain.

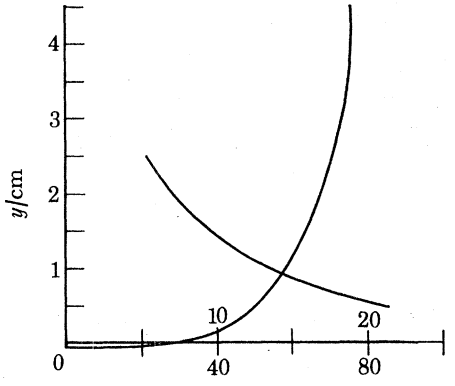

FIGURE 15. The time-mean horizontal velocity profile and velocity gradient du/dy with respect to distance from the bed. $u_* = 6.50$ cm/s; $Y = 4.8$ cm (bed slope = 0.0089).

Some information can however be deduced about body forces other than gravity, by study of the V components only. Figure 13 shows the comparisons between the y displacement of grains falling in still water and the y displacements of grains as they fall from the crest of 22 trajectories. The differences may be attributed to the latter falling through a severe velocity gradient near the bed and thus generating in some way an upward force ignored in a conventional equation of motion.

The effects of turbulence are difficult to isolate, and so only general trends from many observations are of value. Consider first the low trajectories where $y_{\max}$ is less than 1.0 cm (i.e. numbers 3, 4, 7, 10, 11, 12, 17, 19, 20). Five of these nine show a downward acceleration much lower than the still-water case (i.e. numbers 7, 10, 11, 17 and 20). Trajectories 4 and 19 are almost coincident with the still-water plot while numbers 3 and 12 accelerated more slowly from the crest but more quickly near the bed to return approximately to the still-water line. However, in not one of these eight low trajectories does the grain cover the vertical distance from the crest to the bed faster than it would have in still water. Now compare the vertical motion in those trajectories with $y_{\max}$ greater than 1.0 cm. In trajectories 2, 13 and 18 the time to reach the bed was almost exactly the same as it would have been in still water. Trajectories 1, 6 and 14 show the grain to fall faster than the still-water rate, while in the other seven high trajectories the grain fell more slowly. For easy comparison between high and low trajectories it is convenient to use an arbitrary points system: 0 for the same time as the still water case, $+1$ for slower but within 25% of the still water time, $+2$ for slower than 25%, the same negative values for faster than the still-water plot. The results of such a points system is $+4$ over 13 high trajectories and $+8$ over the 9 low trajectories. Thus while both categories of trajectories show by the positive sign that the grains sink more slowly than in still water, the lower trajectories seem to be more marked in this respect than the higher ones. It would therefore appear that an additional upward force acts on the falling grains.

The source of this force might be by repulsion from the bed due to distortions in the flow pattern around grains; by additional drag forces; or by 'shear drift' in the sense first used by Taylor (1917), where a body in a sheared (but non-turbulent) flow has a force on it proportional to the product $(U-u)\,\mathrm{d}u/\mathrm{d}y$.

There are two objections to the suggestion of proximity to the bed causing an upward force on the grain. First, only two trajectories (2 and 13) show reduced vertical accelerations on approaching the bed. Less than 10% can hardly be considered significant. Secondly, Bagnold (1974) showed that although high repulsive forces existed on stationary solid bodies held within one diameter of a solid boundary, these forces seemed to disappear when the body was allowed or caused to rotate. In all of the observed trajectories shown in figure 13 the grain was rotating at a rate comparable with that of the fluid in the velocity gradient, so it would appear that this source of a vertical force is not significant.

Now considering the other two possible sources – the shear drift which will be directed upwards when $U < u$ and downwards when $U > u$; and any addition to the vertical drag force above the drag which would be expected in still water experiments. The total vertical force $F_y = \frac{1}{2}\rho ACV\{(u-U)^2+V^2\}^{\frac{1}{2}}$ (C = drag coefficient on grain of cross-sectional area A) is always larger than for a still water test at velocity V, $F_y = \frac{1}{2}\rho ACV^2$; so an additional upward force is always to be expected (except for the instant $u = U$). Thus in the part of the trajectory between the crest and the place where $u = U$, this additional drag and the shear drift act in the same direction, and discrimination cannot be made between them. Thereafter, as the

grain descends in the velocity gradient, $U > u$, the additional drag force still acts upwards but the shear drift acts downwards. Thus the grain in the latter part of the higher trajectories would fall with more nearly the vertical accelerations experienced in still water. Indeed, evidence from eight of the trajectories show V higher than the still-water speeds.

The shear drift force, proportional to $(U-u)\,\mathrm{d}u/\mathrm{d}y$, gives an explanation of the distinct difference in the rate of fall between high and low trajectories. In the low trajectories the stream had not had sufficient time to accelerate the grain horizontally to the stream velocity at the instantaneous grain height; a plot of U against t usually shows the grain to be accelerating horizontally to the end of the trajectory. Also, the velocity gradients are stronger near the bed than higher in the stream. The result is a lift force which opposes gravity and decreases the downward acceleration of the grain.

In the higher trajectories, the grain has time to approach more closely the same horizontal velocity of the stream. The weaker velocity gradients further from the bed have the dual effect of directly reducing shear drift forces and decreasing $(u-U)$ because of the smaller $\mathrm{d}u/\mathrm{d}y$. The result is an initially small but finite shear drift force directed upwards, followed by zero shear drift as $U = u$, and negative shear drift as $(u-U)$ becomes negative. The effect is illustrated well in trajectories 2, 3, 13, 14 and 18. The arbitrary points allocation shows at a glance that the lower trajectories appear to be held up more than the higher ones.

(*b*) *Elastic rebound from collision with the bed*

Gordon, Carmichael & Isackson (1972), point out that even in an elastic collision between two bodies, the momentum is conserved only if the external forces are small compared with the internal impulsive forces developed by the collision. In this respect it is important to note that in the analysis of our 1000 multi-exposure photographs, many of which involve several contacts with the bed, there was not the slightest evidence of a particle bouncing backwards after a collision. Similarly, Gordon *et al.*, carrying out experiments with vinyl balls in a water-stream, found that generally a moving ball did not bounce off a stationary one, but rolled over it for some distance. They used a flume 0.79 cm wide, with balls 0.664 cm diameter, to ensure a one dimensional situation. The bed was fully mobile. From 21 photographs of collisions in which only one ball was hit they plotted the loss of energy against the striking angle. For a direct head-on collision there was not any bounce, thereby giving a total loss of energy. For a glancing (i.e. tangential) hit, the energy loss is necessarily zero. A straight line was drawn between the above two points when the proportionate energy loss was plotted against the striking angle. The scatter of results is no doubt due to the turbulence in the flow around individual grains of the rough bed, making the grain velocity immediately before and after impact difficult to assess accurately.

In a wide flume, such that the grains are not constricted into one vertical plane, and with non-spherical grains, it appears that there are fewer impacts in which the grain glances off the bed into a low trajectory. The moving grain is able to glance off the sides of the particles into gaps between them. Also, the non-spherical moving grains are less likely to roll around equally non-spherical bed particles after an almost head-on impact; and when a non-spherical grain falls into a rough bed with its long axis vertical there is a large spinning moment exerted on the grain. As this is a form of a glancing blow, there is very little chance of rebound. The grain rolls over the bed particle and is momentarily stopped by the next bed particle before being lifted away again by the flow.

PHILOSOPHICAL TRANSACTIONS OF THE ROYAL SOCIETY A MATHEMATICAL, PHYSICAL & ENGINEERING SCIENCES

In §7, data is presented to show that V at take-off of a trajectory seems rather independent of some prior rolling. Furthermore, table 5 compares y_{max} for trajectories which have started from rest with those starting from a previous impact. Again there is little difference to be found. Thus, it would appear that the trajectory velocities and heights are insensitive to the previous impact history, and it can be inferred that there is no effective elastic rebound between the bed and a moving grain impinging upon it – a point referred to, without proof, by Bagnold (1956, p. 244). It follows that momentum is not conserved at such collisions: the external (fluid) forces acting on the moving grain must be large compared to the internal, impulsive, forces developed by the collision, the latter being effectively damped. The impulsive forces acting on the bed grains must therefore also be negligible; this is of importance in considering the application of our fixed bed experiments to mobile stream beds where the bed grains are all free to move, and where if momentum were so conserved they might be set into motion by impacts. Gordon *et al.*, using free beds, found few cases where an impinging grain dislodged one of the stationary bed grains; and Bagnold (1956) believed that 'Owing to viscous effect in liquids, the grain's velocity on return to the bed is insufficient to cause any observable rebound or any disturbance of the bed grains....' Our initial assumption seems justified; that, by fixing closely graded grains, the motion of moving grains over a plane mobile bed is well modelled. On the other hand previous ideas on saltation have always assumed, from eye observation only, that a grain on impacting a bed immediately starts a new trajectory. The photographic evidence shows otherwise; and thus our saltating grains are rather different from a bouncing ball.

TABLE 6. MEAN LANDING ANGLE OF GRAINS MEASURED FROM TRAJECTORIES

stage	1.04	1.53	1.91	2.52
arctan (leading angle)	0.30	0.26	0.22	0.13

(*c*) *Effective coefficient of friction*, tan α

Table 3 shows how the apparent mean value of tan α increases with stage. This observation should be accepted with reserve, since the method of measurement gives a bias to the results. With trajectories being considered which are only 6 flash intervals (= 0.15 s) or more, the contribution to the mean of tan α from small trajectories is ignored. Thus at low stages only a few trajectories were suitable for analysis by the method given in the appendix, but at high stages most were used to determine the mean. It is to be expected that short trajectories would give high values of tan α, for two reasons. The major reason is seen from figure 14 which shows that the acceleration to a nearly constant U occurs very soon after the start of a trajectory. However, the overall time of the trajectory, Ns, is determined not so much by U as by the initial vertical velocity V_1, which impels the grain to a larger height. So with $\tan\alpha = (U_2 - U_1)\,Ns$, a short trajectory with small Ns will inevitably give a large tan α. Secondly, short trajectories have rather larger landing angles (table 6) than those of longer trajectories, again shown by the mean geometry $\bar{L}/\bar{y}_{max}$ of figure 5. These larger landing angles cause the grain to sustain a larger x-deceleration on striking the bed, giving a smaller U_1 in the next trajectory and so a larger tan α for it. This is also described in §9(*b*).

It is therefore to be expected that tan α, as measured by our technique, is always underestimated but with the greatest error at low stages. The true value would seem to be distinctly higher than the 0.63 assumed in Bagnold (1973) on the basis of earlier indirect evidence.

Further improvement of knowledge of this parameter awaits better photographic technique to obtain grain positions more closely spaced, without the difficulties of overlapping images.

(*d*) *Occurrence of modes of transport*

The boundaries of the modes, figure 1, show the markedly different shape of the rolling/saltation boundary compared to that of the saltation/suspension boundary. These boundaries must be considered in the light of the definitions of §4 and the photographic limitations of the 0.025 s flash intervals. Noting that the zero for the rolling curve is at the top of the diagram, it is seen that the percentage of time spent in rolling decreases very quickly from 60 % near the threshold to 20 % at $u_*/u_{*0} = 1.4$. At $u_*/u_{*0} = 3.0$ only 3 % of the time is spent rolling. The rather fast decrease in the occurrence of rolling in the range $1.0 < u_*/u_{*0} < 1.2$ can be attributed to several co-existing causes:

(i) The subsidiary experiments where a grain started from rest show that the mechanism of lifting a grain does not depend on elastic rebound. For rolling, the local u velocity near the grain must be just large enough to provide a driving force; yet u must be low to avoid the probability of an upward fluid impulse by a velocity v'. Thus, the probability of there being sufficiently low fluid velocity over the grain so as to roll it but not to start a saltation is greatly reduced as the stage increases from 1.0.

(ii) Saltation grains follow trajectories which increase both in L and in time as the stage increase; the number of impacts with the bed therefore decreases, and so does the opportunity for the grain to roll.

(iii) With increase of u_*/u_{*0}, there is also a decrease in the angle with which the grains strike the bed at the end of a trajectory. Table 6 (§9(*c*)) showed some average angles from selected runs.

The small angles give a smaller chance that the grain strikes the bed nearly 'head-on' with the associated large loss of kinetic energy; there is a larger chance of a glancing blow, and so less chance of a subsequent roll.

The much less abrupt curve defining the boundary between saltation and suspension in figure 1 shows a less rapid development of the suspensive mode than the development of the saltation mode. Figure 1 shows the percentage of *time* in the indicated mode, and not the number of times the particular mode occurs. There is a small proportion of suspension observed at very low stages. So, even at very low u_*/u_{*0}, with short trajectories, there are a small number of turbulent and upward impulses large enough to cause a resultant upward force on the grain indicated by upward accelerations (figure 2). At higher u_*/u_{*0} there are more and stronger v', and the probability of a grain being accelerated upwards when not in contact with the bed is thereby greatly increased. Since it is the resultant upward force on a grain which must be positive to produce an upward acceleration, there is a much greater chance of suspension during the falling portion of the trajectory than during the rising portion. On the rising part, both the vertical component of the drag force and the gravitational force are directed downwards so the vertical components of turbulent velocity to cause suspension, v', must be relatively large. At the top of the trajectory, however, where the vertical component of the drag force is zero, v' now needs to be much less to overcome gravity. During the falling part of the trajectory, as the vertical component of drag increases in an upward direction, gravity is more nearly balanced, and still smaller v' will cause suspension within the definition of §4.

As the stage increases three additive changes take place. First, V, just before hitting the bed, increases, since the trajectories have become higher: and this serves to increase the vertical drag force which opposes gravity and reduces v' required to cause suspension. Secondly, the intensity of v' increases with u_*. And thirdly, with increase of u_*/u_{*0}, the impulses just large enough to cause suspension appear further inwards from the thin tail of their frequency distribution curve of v'. All these effects result in a much larger possibility of suspension.

(e) *Dependence of saltant trajectories on stage*

The curves of figures 1, 3 and 4 show various statistics of *saltant* trajectories from the experiments of set 2 grains of different densities, all at $Y = 4.82$ cm. Figure 12 gives similar information for $Y = 7.2$ cm and it is clear that these statistics depend only on stage, and not on density ρ_g or Y. Suspensive trajectories are not so independent and are further discussed in §9(i).

Within the bounds of our experiments with one shape and size of grain, figure 3 shows how $\bar{y}_{\max}$ depended only on u_*/u_{*0}. Thus in the rising part of the trajectory, the effect on $\bar{y}_{\max}$ of the upward impulses on a grain (controlled by u_*) seems to prevail over any systematic variation in vertical drag forces (shown in §9(*a*) to be partly controlled by $|u-U|$). If this is accepted, it is not so clear that $\bar{L}$ necessarily also depends on u_*/u_{*0}, even though empirically it is shown in figure 4 to be so, since the horizontal velocities U (which control the x-displacements of a trajectory) depend, in turn, on conditions in the stream remote from the bed. So first considering the falling part of the trajectory, where V is negative and increasing: there is insufficient time for the grain to achieve its steady V_g (which is already established to be proportional to its u_{*0}). However, the subsidiary experiment in which grains were allowed to fall freely from rest in water discloses (table 7) that the time for a 1 cm ($= 2.5D$) drop is inversely proportional to u_{*0}. So, approximating the fall of the grain from the trajectory crest to the fall in still water, the time required for a fall from $y_{\max}$ will therefore depend on $y_{\max}$ and $1/u_{*0}$. But $y_{\max}$ is already accepted as a function of stage (figure 3), thus the time for the fall from $y_{\max}$ is a function of stage and $1/u_{*0}$.

TABLE 7. SUBSIDIARY EXPERIMENT – GRAINS SETTLING FROM REST IN STILL WATER

grain density	u_{*0}/(cm s^{-1})	time for 1 cm fall/s	time, $\times u_{*0}$/cm
1.20	2.763	0.118	0.326
1.26	3.147	0.114	0.359
1.43	4.008	0.086	0.344
2.49	7.496	0.045	0.336
2.88	8.420	0.041	0.344

Suppose also that the time for the rising portion of the trajectory depends on u_{*0}, it then follows that the mean time of the whole trajectories T is a function of stage and of u_{*0}, i.e. $T = (1/u_{*0})\, f(\text{stage})$. Now consider the distance travelled horizontally, during the time of the trajectory. Most of the horizontal acceleration takes place in a short distance at the beginning of the trajectory, so U is therefore closely related to the mean velocity of the fluid layer u in which the trajectory occurs. Due to the logarithmic velocity distribution appropriate to a rough bed, u is dependent on u_*, but is only weakly dependent on the height of the layer, which has at its limit $y_{\max}$.† The horizontal distance L travelled by a trajectory, nearly

† A layer from $y = \frac{1}{2}D$ to $y = 2D$ has a mean u velocity only 15% greater than one from $y = \frac{1}{2}D$ to $y = D$. A deeper layer to $y = 4D$ (a very high trajectory in our case) gives this mean u velocity 32% greater at the same u_*.

proportional to T and the mean velocity within the layer defined by y_{max}, is therefore

$$L \propto Tu_*,$$

and substituting $T = 1/u_{*0}f$ (stage), gives

$$L = \left\{\frac{1}{u_{*0}} f\,(\text{stage})\right\} u_*$$

or

$$L = f_1\,(\text{stage}).$$

In fact figure 4, with figure 12, show L to be determined only by u_*/u_{*0}, and, within our range of the variables, independent of Y and ρ_g. There appears to be no effect of D but our range of this variable is small (table 1).

(*f*) *Dimensions of trajectories*

Figure 3 shows the mean values of y_{max} for suspensive trajectories to increase with stage, but the saltant trajectories show a similar increase only to stage 2.3, when a maximum is reached at a value of $y_{max} = 1.44$. If y_{max} increases then both the time of descent from the top of the trajectory and the vertical velocity on landing (if less than V_g) will both increase. The latter causes a larger drag force opposing gravity so that a smaller v' is needed to give an upward acceleration. Both of these factors increase the chance of a sufficiently high v' to cause the grain to become suspended. As the turbulence intensity increases with increasing stage, only the lower trajectories where the probability of becoming suspensive is not as great retain their saltant classification, so that $\bar{y}_{max}$ for saltations falls.

The same form is seen in figure 4 for $\bar{L}$ where after the same stage of 2.3 the saltation length is seen to decrease with increasing stage. There is no such maximum for the suspensive trajectories, which continue to increase in length with stage. Since L can be assessed only from complete trajectories in which the impacts with the bed at the beginnings and ends are both registered, less data is available than in the case of y_{max} where the ends of the trajectories could be neglected, provided a maximum height was recorded. It becomes evident that $\bar{L}$ at the higher stages is systematically underestimated by the analysis technique, since many of the longer trajectories start or finish outside the field of view of the camera. Therefore, the shorter trajectories are more likely to be measured, giving a low value for $\bar{L}$, with the error increasing with $\bar{L}$.

Figures 3 and 4 have been combined in figure 5, which demonstrates how the geometric similarity of trajectories changes with stage and the onset of suspension. If the trajectory shape were the same for all stages, the two lines in figure 5 would be parallel, which is almost so until stage 1.5. However, as suspension progresses, y_{max} of any trajectory cannot go greater than the depth of the stream. Since a neutrally buoyant grain (i.e. a flow tracer; and so by definition a stage tending to infinity) will not necessarily always reach the water surface between successive contacts with the bed the mean value, $\bar{y}_{max}$, will become asymptotic to some value less than the depth Y. On the other hand, there is no such limit to $\bar{L}$, which at large stages will tend to an indefinite and very high value. Therefore, there cannot be geometric similarity between $\bar{y}_{max}$ and $\bar{L}$ at stages which include much suspension.

The frequency distributions of y_{max} for grains at the same stage but of different densities, as shown in figure 7 give a distinction between grains of the same size and shape but of different eight. It would appear that beca use the means of the two distributions are identical, $\bar{y}_{max}$

is uniquely dependent on u_*/u_{*0} and independent of ρ_g, a point already made by figure 1. However, the less peaked distribution of y_{max} for heavier grains at the same u_*/u_{*0} is contradictory, and implies that the effect of increased stream turbulence with increasing u_* to be dispersive of y_{max}, while not affecting $\bar{y}_{max}$. This can be explained on the basis of the lift force on the grain (which controls y) being almost impulsive at the beginning of the trajectory, and hydrodynamic in origin; thus it would depend on the instantaneous horizontal velocity $u+u'$, and not on v' (which is small near the bed). The horizontal velocities have little subsequent effect on the suspensive properties; but the wider range of u' at higher flows (having the same stage as lower flows with lighter grains) results in a more widely spread distribution of y_{max} for the heavier grains. In our observations, due to the relatively long flash interval of $\frac{1}{40}$ s imposed on us by photographic restriction, these impulsive accelerations could not be detected from the grain-image positions.

Figures 8*a* and *b*, each at one stage, indicate another aspect of geometric similarity of trajectories. At the higher stage, with much suspension, the dispersion of data is large: the photographs showed many part-trajectories of which neither y_{max} nor L could be determined. The suspensive trajectories are therefore noticeably more dispersed than the saltant ones, and are generally longer for the same height. At the lower stage, 1.53, the results form a narrower band, with the saltations very nearly similar in geometry.

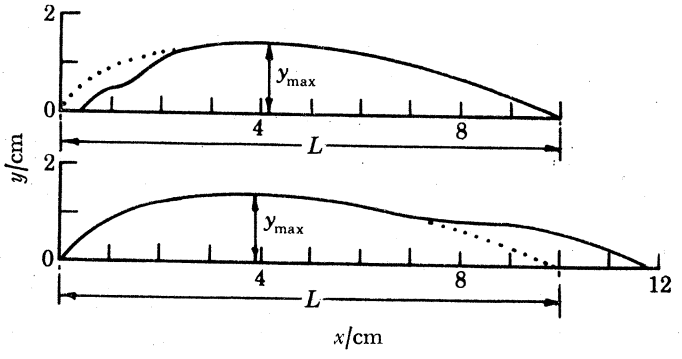

FIGURE 16. Comparison of two types of suspensive trajectories. (*a*) Impulse received before the crest; (*b*) Impulse received after the crest. In each case the dotted line indicates a typical saltation of the same y_{max} which would have occurred if the impulse had not been present.

The small group of four low saltations are no doubt the result of glancing impacts on the bed where a significant portion of the forward speed was conserved. The suspensive trajectories are seen to plot predominantly to the right-hand side of the figure. A grain which receives a suspensive impulse after y_{max} has been recorded is then carried further downstream before hitting the bed. A much smaller number of suspensive trajectories lie to the left of the bulk of results. It is evident that if a vertical acceleration from turbulence occurs during the rising part of the trajectory, then y_{max} will be increased, but with L being increased only during the falling portion. During its ascent the grain will have travelled a shorter horizontal distance than it would have to reach the same height in a saltation (figure 16). The result confirms the conclusions, drawn in §9(*d*), that the chance of suspension occurring during the falling part of the trajectory is higher than during the rising part.

Similar results have also been plotted for lower stages (although not presented here), where it was seen that especially for the lower trajectories there was even more dispersion. The irregularities of the contact with the bed is probably the direct cause.

(g) *The centre of thrust* y_n

This parameter, defined as

$$y_n = \frac{1}{U_2 - U_1} \int_{U_1}^{U_2} y \, \mathrm{d}U,$$

is the height at which the effective forward thrust is applied to the grain during a saltation. The 30 values of $y_n/y_{\max}$ from individual trajectories at $u_*/u_{*0} = 1.53$ gives a mean of 0.836, and show the scatter of figure 9; there are no values lower than $y_n/y_{\max} = 0.6$, but several exceed 1.0. The high values are associated with trajectories in which a falling grain is considerably decelerated to give low $U_2 - U_1$. Reference to a diagram, figure 17, in the $y-U$ plane reveals that a grain accelerated while it is rising to $y_{\max}$, and then decelerated at nearly the same rate gives low $U_2 - U_1$, but $y_n/y_{\max}$ approaches 1.0; a decrease in the last few milliseconds to make $U_2 - U_1$ still smaller will make $y_n/y_{\max} > 1.0$. In contrast, a grain which is further accelerated in descent, giving a triangular $y-U$ diagram and a large $U_2 - U_1$ produces $y_n/y_{\max} = 0.5$. To obtain a still lower value, there would need to be a considerable x acceleration near the bed.

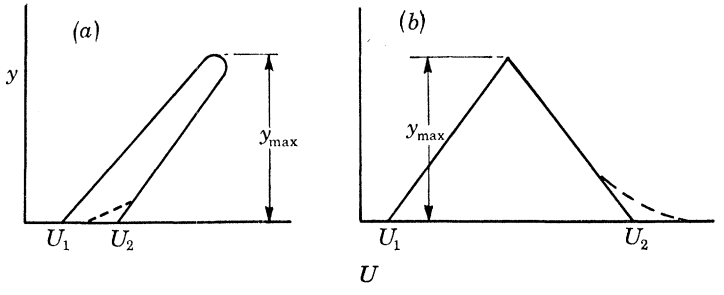

FIGURE 17. Diagram to show two contrasting ways in which grain trajectories may plot on the y–U plane
(*a*) Grain acceleration in x direction is followed approximately by similar deceleration. Thus

$$y_n = \frac{1}{(U_2 - U_1)} \text{(area under curve)} = \frac{(U_2 - U_1)\, y_{\max}}{(U_2 - U_1)} = 1.0 y_{\max}.$$

Observe that if there is a last-moment deceleration near the bed, shown by dotted line, $y_n > 1.0 y_{\max}$.
(*b*) Grain acceleration is followed by continued acceleration. Thus

$$y_n = \frac{\frac{1}{2}(W_2 - U_1)\, y_{\max}}{(U_2 - U_1)} = 0.5 y_{\max}.$$

Observe that last-moment acceleration near the bed gives $y_n < 0.5 y_{\max}$.

It is of interest to observe that none of the 30 trajectories gave $y_n/y_{\max} < 0$ so that the accelerations near the bed on a descent are remarkably absent. On the other hand it is equally surprising to find 8 of the 30 with $y_n/y_{\max} > 0.9$: it is therefore much more common to find low-speed fluid near the bed than it is to find high speed 'gusts' brought down by turbulence from the higher mean velocities in the upper parts of the stream. Such a conclusion is, of course, in accordance with recent ideas on the structure of turbulence over rough surfaces, where sudden, high velocity 'bursts' or inclined jets have been measured with more sophisticated equipment than our grains.

(h) *Mean forward speed of grains* $\bar{U}$

The mean forward speed, $\bar{U}$, for a single grain in all modes of motion is shown, in figure 11, to be linearly dependent on u_* for a particular stream depth, over a wide range of transport

stage (0.78–3.05). At the lower limit, the grain would be rolling in contact with the bed for 90—100 % of the time. Conversely, at the upper limit the grain will be travelling in a suspensive mode for almost 95 % of the time. Although at first it may seem surprising that a linear relation should exist over our 3-fold range of u_* (i.e. 9-fold range of τ) when such different modes occur, it should be remembered that our definition of suspension does not carry the implication of positive V and so of full suspension. Fine grains in rivers, when in a fully suspensive mode are at much higher u_*/u_{*0} than our experiments. Thus the lines of figure 11 may only be tangents at the lower ends of more complex curves. When trajectories are only saltations, as discussed in §9 (*e*), all motions including $\bar{U}$ are likely to be dependent on u_* alone, and the linear relationship for $\bar{U}$ is to be expected. It seems that the degree of suspension found in our experiment does not greatly distort this simple law.

While the ratio V_g/u_* is a useful *approximate* parameter for correlating all values of $\bar{U}/\bar{u}$, Francis (1973), our tests reported here show a certain scatter when plotted in this way – heavy grains having a smaller $\bar{U}/\bar{u}$ at a given V_g/u_* than light grains. So V_g does not seem wholly to correlate the effect of ρ_g. Some light is thrown on this effect in the following way:

On figure 11, the lines for different ρ_g can be written

$$\bar{U} = b(u_* - f(\rho_g)), \tag{1}$$

where $f(\rho_g)$ is a function of grain density and b is a constant for each set of grains but which may vary with different grain shapes and sizes.

Now the values of u_{*0} used for other statistics were calculated from Shields (1936) with a value of 0.06 assigned to the non-dimensional shear parameter θ_0. This assumes the simple grain is coplanar with a bed of loose grains similar to itself. It has been found, however, in experiments with these same grains (Fenton 1976) that if the single grain is placed in an overriding position on top of fixed bed grains as it indeed is placed in our experiments, then θ_0 is as low as 0.02. Recalculating the critical shear velocity, calling it now u_{*1}, with $\theta_0 = 0.02$, gives values which are identical to the shear velocities found by extrapolation to the $\bar{U} = 0$ axis in figure 11, and so show in equation (4) that $f(\rho_g) = u_{*1}$. Substitution gives

$$\bar{U} = b(u_* - u_{*1}). \tag{2}$$

Similar relationships between $\bar{U}$ and u_* were found for the other sets of grains with little variation in the value of b. A maximum of $b = 14.3$ was found for the set 3 spheres, and a minimum $b = 13.5$ was found with some tests on angular chips of crushed granite. The values for sets 2 and 3 grains were $b = 13.8$ and 13.85 respectively.

Now considering the arrangement of parameters $\bar{U}/\bar{u}$ against V_g/u_* as used by Ippen & Verma (1953) and Francis (1973), each variable may be considered in turn:

(i) $\bar{U}$ is given by equation (2).

(ii) For fully developed turbulent flow the well-known equation can be written for mean stream velocity, i.e.

$$\bar{u}/u_* = 5.75 \lg (Y/D) + 6, \tag{3}$$

which for constant Y over the same bed reduces to

$$\bar{u} = cu_*, \quad \text{where} \quad c = \text{constant}. \tag{4}$$

(iii) From Francis (1973) it was shown $u_{*0}/V_g = (\frac{3}{4}\theta_0 C)^{\frac{1}{2}}$ so that for any one grain (using u_{*1} for u_{*0} merely changes the constant)

$$V_g = au_{*1}, \quad \text{where} \quad a = \text{constant}. \tag{5}$$

PHILOSOPHICAL TRANSACTIONS OF THE ROYAL SOCIETY A MATHEMATICAL, PHYSICAL & ENGINEERING SCIENCES

Substituting the equations (2), (4) and (5) for the original parameters of equation (1) and making $\bar{U}/\bar{u} = P$, $au_{*1}/u_* = Q$, then

$$P = \frac{b}{c}\left(1 - \frac{Q}{a}\right), \tag{6}$$

which is a straight line of negative slope b/ac, intersecting the P and Q axes at b/c and a respectively.

From V_g (table 1) and u_{*1}, a can be calculated: while the approximation of a constant for a was good for spheres, more irregular grains (which rotated as they fell in still water) gave smaller values of a as ρ_g increased. For example set 3 grains gave $a = 10.17$, 8.72, 8.58, 9.11, 7.43 and 7.78, for the range of ρ_g in table 1 ($1.20 < \rho_g < 2.60$). Putting $D = 0.85$ and $Y = 4.8$ cm in equation (3) gives $c = 10$.

Now putting $b = 13.8$, $c = 10$, with the relevant values of a, equation (6) can be drawn for each grain, forming the straight lines of figure 18. In addition, the experimental points

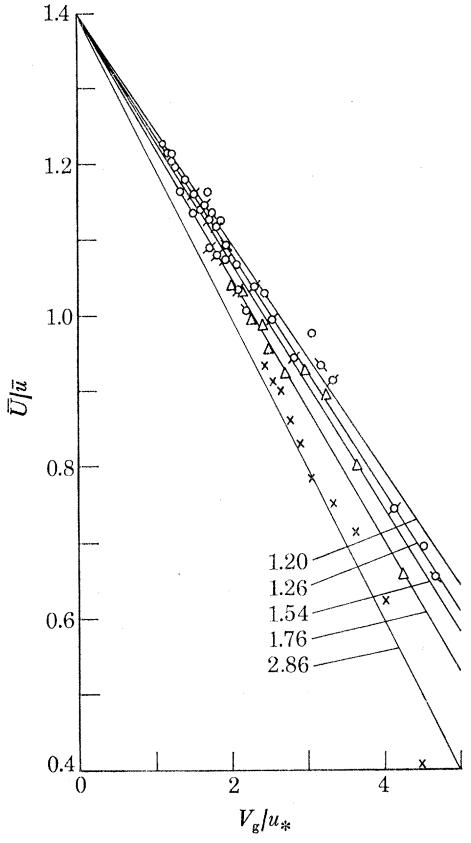

FIGURE 18. Plot of the theoretical equations (6) using values of constants a, b, c, as detailed in text. Experimental values of $\bar{U}/\bar{u}$ and V_g/u^* superimposed from figure 11.

from figure 11 have been replotted in the form $\bar{U}/\bar{u}$ against V_g/u_*. It is clear that the data now follows the straight lines, and that there is a systematic variation between grains of different ρ_g, and therefore V_g. By not separating these families of straight lines, a single and slightly curved line could justifiably be drawn through the points, as was done in the original observation of Ippen & Verma (1953) and Francis (1973). The changes in a, which cause the above

systematic variation may be due to the spin of the grains relative to the water stream. Terminal velocity determinations in still water revealed that the heavier grains had a greater tendency to spin than lighter grains; and that when they did so, V_g was smaller (i.e. a smaller) than when they fell without spinning.

(i) *Effect of stream depth Y*

The effect of changing the depth from $Y = 4.8$ cm to $Y = 7.2$ must be considered bearing in mind changes in the $\bar{u}$ profiles. From the well-known equation (3) for the time-mean velocity $\bar{u}$ at a height y above the bed, u should be independent of Y for a constant roughness and u_*. In our tests, measurement of two velocity profiles both at $u_* = 7.9$ cm/s – one at $Y = 4.8$ cm, the other at $Y = 7.2$ cm, showed complete coincidence for the 4 cm nearest the bed.

With the above considerations on the time-mean horizontal velocity $\bar{u}$, it is not at all surprising that saltations, all within the lowest layer of the flow, are seen to be little affected in either $\bar{y}_{\max}$ or $\bar{L}$ by a change in depth. It is striking, however, that with suspensive trajectories both $\bar{L}$ and $\bar{y}_{\max}$ are increased by an increase in Y for all stages. It is also apparent that rolling is slightly decreased and that the frequency of suspension significantly increased at the higher stages. This evidence points to a change in the structure of turbulence in the flow with a change in depth within the limits of the experiments $5.8D < Y < 8.8D$. A decrease in the rolling mode is dependent not on the time-mean velocity $\bar{u}$, but on the instantaneous horizontal velocity $\bar{u}+u'$ when the grain is in contact with the bed. The increase in the frequency of suspensions can be attributed only to higher positive v'. It must be remembered that measurements of trajectories were made with grains moving in the centre portion of the channel. Since the bed roughness was not changed, increasing Y without altering the width will have the effect of increasing the ratio of wall drag to that of the bed. The possibility of the associated increase in secondary velocities superimposed on v' could account for some of these experimental observations.

The changes of Y, however, made little change in $\bar{U}$ as shown in figure 12, despite the increase in the mean height of the grain, and the associated more frequent suspensions: with grains being higher, and so affected by fluid velocities which are themselves greater, a rather higher $\bar{U}$ would be expected. The effect is small. At $u_*/u_{*0} = 2.5$, from figure 6, for a change of Y from 4.8 to 7.2 cm, $\bar{y}$ changes only from 1.2 cm ($= 1.45D$) to 1.42 cm ($= 1.71D$) above the bed. In a logarithmic velocity profile, governed by a roughness size $k = D$, u at these heights changes by 6 %. The maximum heights of trajectories, even when suspensive, change less, in this case only from 1.76 to 1.92 cm; the velocities here change by only 2 %. The suspensions, more frequent in the tests at greater depth, are characterized by longer and flatter trajectories, and so the grains are more affected by fluid speeds at the crests than by the speeds near the bed in which they are travelling for a much shorter time. Such a small effect on $\bar{U}$, if present, was not observable by our methods of measurement.

10. Summary of conclusions

In both high and low trajectories, grains fall from a crest with an initial acceleration less than that in still water, due to the drag of the relative velocity $|U-u|$; in low trajectories, which have stronger velocity gradients near the crests, grains fall much more slowly than they do in high trajectories. This is explained by the shear drift force.

PHILOSOPHICAL TRANSACTIONS OF THE ROYAL SOCIETY A MATHEMATICAL, PHYSICAL & ENGINEERING SCIENCES

There appears to be no effective elastic rebound between the bed and a moving grain impinging on it. The fixing of bed grains must therefore have little effect on moving grains compared to the latter's motion on a fully mobile grain bed.

The mean value of tan α is underestimated by the photo technique but seems to be distinctly higher than 0.63 previously assumed.

The boundary curves for different modes of motion show that at the highest stages of the tests, there is still a significant amount of rolling motion, even though suspensive trajectories then predominate.

Dimensions of the saltant trajectories are determined by stage for a given grain size, and are independent of grain density and stream depth.

The geometric similarity of trajectories changes with stage and the onset of suspension.

In saltations, $\bar{y}_{\max}$, $\bar{L}$ and $\bar{U}$ are all dominated by u_*/u_{*0}, the effects of Y being insignificant. In suspensive trajectories, however, $\bar{y}_{\max}$ and $\bar{L}$ increase with Y.

The chance of suspensive effects occurring during the falling part of a trajectory is higher than during the rising part.

The mean centre of thrust y_n is about 84 % of $y_{\max}$ at $u_*/u_{*0} = 1.5$, but the range of values in different trajectories is high.

Near the bed, it is much less common to find relatively high fluid speeds, of a magnitude sufficient to affect the grain speed in a downstream direction, than it is to find low speeds.

The grain speed averaged over several trajectories $\bar{U}$, divided by the time-space mean water speed $\bar{u}$, is related to V_g/u_* by a family of straight lines, each line for a different ρ_g. Over the range of experiments, $\bar{U}$ was proportional to $u_x - u_{x1}$.

This work was carried out with the aid of a Research Grant from the Natural Environment Research Council, London.

References

Abbott, J. E. 1974 The dynamics of a single grain in a stream. Ph.D. thesis, University of London.

Bagnold, R. A. 1956 The flow of cohesionless grains in fluids. *Phil. Trans. R. Soc. Lond.* A **249**, 235–297.

Bagnold, R. A. 1973 The nature of saltation and of 'bed-load' transport in water. *Proc. R. Soc. Lond.* A **332**, 473–504.

Bagnold, R. A. 1974 Fluid forces on a body in shear-flow; experimental use of 'stationary flow'. *Proc. R. Soc. Lond.* A **340**, 147–171.

Fenton, J. & Abbott, J. E. 1977 Initial movement of grains on a stream bed: the effect of relative protrusion. *Proc. R. Soc. Lond.* A **352**, 523–537.

Francis, J. R. D. 1973 Experiments on the motion of solitary grains along the bed of a water-stream. *Proc. R. Soc. Lond.* A **332**, 443–471.

Gordon, R., Carmichael, J. B. & Isackson, F. J. 1972 Saltation of plastic balls in a 'one-dimensional' flume. *Water Resources Res.* **8**, 444–459.

Ippen, A. T. & Verma, R. P. 1953 Motion of discrete particles along the bed of a turbulent stream. *Proc. Minnesota Int. Hydraulics Convention.*

Shields, A. 1936 *Preus. Versuchs...Schiffban, Berlin*, 1936; translated and quoted in *Loose boundary hydraulics* (ed. A. J. Raudkivi), pp. 21–17. London: Pergamon Press.

Taylor, G. I. 1917 Motion of solids in fluids when the flow is not irrotational. *Proc. R. Soc. Lond.* A **93**, 99–113.

PHILOSOPHICAL TRANSACTIONS OF THE ROYAL SOCIETY A MATHEMATICAL, PHYSICAL & ENGINEERING SCIENCES

Appendix. The effective angle of friction α, and the centre of thrust y_n

Just before an impact of a grain with the bed, U is larger than just after an impact. There must have been a retarding force on the grains and the ratio of this force to the downward gravity force on it can be regarded as a coefficient of friction, $\tan\alpha$. In a steady motion the mean retarding force exactly equals the mean forward fluid thrust during the trajectories and this can be estimated by the acceleration of the grain to the final speed U_2 just before impact.

Thus in a trajectory in which $N+1$ images of the grain were photographed, time T was Ns, where s is the $\frac{1}{40}$ s flash interval. Extrapolation of the grain image positions backward to contact with the bed gives generally a non-integral value of N, and gives more accurate estimates of U_1 and U_2 than were possible by the rather crude analysis given by Francis (1973). Measurement of U_1 and U_2 was made by taking the horizontal distances x_1 and x_2 on the photographs between extrapolated impact positions and the second image after (for U_1) or before (for U_2) impact.

The initial velocity component is thus $U_1 = x_1/\mathrm{s}$; and the final velocity component is $U_2 = x_2/\mathrm{s}$. The streamwise impulse gained is $M(U_2-U_1)$ and the mean fluid thrust over the whole trajectory on the grain of mass M is

$$M(U_2-U_1)/Ns.$$

Since the normal gravity force on a grain is

$$Mg(\rho_g-\rho)/\rho_g$$

the coefficient of friction is

$$\tan\alpha = M(U_2-U_1)/Ns\left(\frac{\rho_g-\rho}{\rho_g}\right)Mg$$

$$= (x_2-x_1)/Ns^2\left(\frac{\rho_g-\rho}{\rho_g}\right)g.$$

The forward fluid thrust on a grain may be assumed to be a function of the fluid velocity at the grain-centre height y. Thus a mean effective fluid velocity will be that at a height y_n, where

$$y_n = \frac{1}{(U_2-U_1)}\int_{U_1}^{U_2} y\,\mathrm{d}U.$$

This parameter may be obtained by a graphical integration $\int y\,\mathrm{d}U$, with data for y and U found from the photographs.

PHILOSOPHICAL TRANSACTIONS OF THE ROYAL SOCIETY A MATHEMATICAL, PHYSICAL & ENGINEERING SCIENCES